Carbon emission limits required to satisfy future representative concentration pathways of greenhouse gases

V. K. Arora,[1] J. F. Scinocca,[1] G. J. Boer,[1] J. R. Christian,[1,2] K. L. Denman,[1,3] G. M. Flato,[1] V. V. Kharin,[1] W. G. Lee,[1] and W. J. Merryfield[1]

Received 1 December 2010; revised 3 February 2011; accepted 7 February 2011; published 10 March 2011.

[1] The response of the second-generation Canadian earth system model (CanESM2) to historical (1850–2005) and future (2006–2100) natural and anthropogenic forcing is assessed using the newly-developed representative concentration pathways (RCPs) of greenhouse gases (GHGs) and aerosols. Allowable emissions required to achieve the future atmospheric CO_2 concentration pathways, are reported for the RCP 2.6, 4.5 and 8.5 scenarios. For the historical 1850–2005 period, cumulative land plus ocean carbon uptake and, consequently, cumulative diagnosed emissions compare well with observation-based estimates. The simulated historical carbon uptake is somewhat weaker for the ocean and stronger for the land relative to their observation-based estimates. The simulated historical warming of 0.9°C compares well with the observation-based estimate of 0.76 ± 0.19°C. The RCP 2.6, 4.5 and 8.5 scenarios respectively yield warmings of 1.4, 2.3, and 4.9°C and cumulative diagnosed fossil fuel emissions of 182, 643 and 1617 Pg C over the 2006–2100 period. The simulated warming of 2.3°C over the 1850–2100 period in the RCP 2.6 scenario, with the lowest concentration of GHGs, is slightly larger than the 2°C warming target set to avoid dangerous climate change by the 2009 UN Copenhagen Accord. The results of this study suggest that limiting warming to roughly 2°C by the end of this century is unlikely since it requires an immediate ramp down of emissions followed by ongoing carbon sequestration in the second half of this century.
Citation: Arora, V. K., J. F. Scinocca, G. J. Boer, J. R. Christian, K. L. Denman, G. M. Flato, V. V. Kharin, W. G. Lee, and W. J. Merryfield (2011), Carbon emission limits required to satisfy future representative concentration pathways of greenhouse gases, *Geophys. Res. Lett.*, *38*, L05805, doi:10.1029/2010GL046270.

1. Introduction

[2] The climate model simulations for the fifth assessment report (AR5) of the Inter-governmental Panel on Climate Change (IPCC) are based on the newly-developed representative concentration pathways (RCPs) of radiatively important greenhouse gases (GHGs) (http://www.pik-potsdam.de/~mmalte/rcps/index.htm). Historical (1850–2005) and future (2006–2100) simulations based on these RCPs are a key element of the upcoming fifth Coupled Modeled Intercomparison Project (CMIP5, http://cmip-pcmdi.llnl.gov/cmip5/forcing.html). The RCPs, which are based on simulations from a set of integrated assessment models (IAMs), provide both concentrations and emissions of radiatively important GHGs, emissions of several aerosols and their precursor species, and associated land cover change scenarios (http://luh.unh.edu/). A central focus of the AR5 effort involves next-generation experiments in which earth system models (ESMs) are run with scenarios of prescribed concentrations of GHGs that lead to the stabilization of radiative forcing to different levels at, or sometime after, the end of this century. Driven with specified concentration of CO_2 (and other GHGs) in this way, ESMs yield atmosphere-land and atmosphere-ocean carbon fluxes that may be used to obtain an inverse estimate of the anthropogenic emissions required to achieve a given CO_2 pathway [*Hibbard et al.*, 2007]. Here, we summarize the physical and biogeochemical response of the second-generation Canadian earth system model (CanESM2) to historical (1850–2005) and future RCP-based (2006–2100) prescribed CO_2 and other GHGs forcing, focusing in particular on inverse estimates of allowable emissions. These results will soon be available as part of the CMIP5 project and will contribute to the fifth assessment report of the IPCC.

2. Model Description and Experimental Set Up

[3] CanESM2 has evolved from the first generation Canadian earth system model (CanESM1) [*Arora et al.*, 2009; *Christian et al.*, 2010] of the Canadian Centre for Climate Modelling and Analysis (CCCma). The atmospheric component of CanESM2 (CanAM4) has evolved from the third generation atmospheric general circulation model (CanAM3) [*Scinocca et al.*, 2008]. It is a spectral model employing T63 triangular truncation with physical tendencies calculated on a 128 × 64 (~2.81°) horizontal linear grid. The physical ocean component of CanESM2 differs from that of CanESM1 in that it has higher resolution and improved physical parameterizations. Changes to the physical atmosphere and ocean components of CanESM2, compared to CanESM1, are summarized in the auxiliary information.[1] The effects of explosive volcanoes for the 1850–2005 period is included by prescribing stratospheric aerosol distribution following the CLIVAR C20C protocol (http://www.iges.org/c20c/). Solar variability is included for the period 1850–2005 following CMIP5 recommendations (http://www.geo.

[1]Canadian Centre for Climate Modelling and Analysis, Environment Canada, University of Victoria, Victoria, British Columbia, Canada.
[2]Also at Fisheries and Oceans Canada, Institute of Ocean Sciences, Sidney, British Columbia, Canada.
[3]Also at VENUS, University of Victoria, Victoria, British Columbia, Canada.

[1]Auxiliary materials are available in the HTML. doi:10.1029/2010GL046270.

fu-berlin.de/en/met/ag/strat/forschung/SOLARIS/Input_data/CMIP5_solar_irradiance.html) and is extended into the future by repetition of the last solar cycle (1997–2008).

[4] The ocean and land carbon cycle components of CanESM2 are essentially the same as those in CanESM1 and are represented by the Canadian Model of Ocean Carbon (CMOC) [*Christian et al.*, 2010, and references therein] and the Canadian Terrestrial Ecosystem Model (CTEM) [*Arora et al.*, 2009; *Arora and Boer*, 2010], respectively (see auxiliary information). Land use change (LUC) emissions are interactively modelled on the basis of changes in land cover [*Arora and Boer*, 2010] which yields land-atmosphere CO_2 fluxes that are consistent with historical changes in crop area. This approach is superior to the direct injection of LUC emissions into the atmosphere (e.g. similar to fossil fuel emissions) with no corresponding changes at the land surface, which does not take into account the associated albedo changes or the reduced capacity of the biosphere to sequester carbon. This is especially important when natural vegetation is replaced with croplands. The historical land cover is reconstructed following *Arora and Boer* [2010] on the basis of historical changes in crop area provided in the CMIP5 dataset. A similar approach is used for future land cover based on changes in crop area associated with each RCP scenario.

[5] The vertically integrated globally-averaged carbon budget equation for the atmosphere as modeled here is

$$\frac{dH_A}{dt} = E_F - F_O - F_L = (E_F + E_{LUC}) - F_O - F_{Ln} \qquad (1)$$

where H_A is the global atmospheric carbon burden (Pg C), F_O and F_L are the atmosphere-ocean and atmosphere-land CO_2 fluxes (Pg C/yr), respectively, and E_F is the anthropogenic fossil fuel emissions (Pg C/yr). The modeled atmosphere-land CO_2 flux ($F_L = F_{Ln} - E_{LUC}$) is made up of the natural component (F_{Ln}) and the interactively modeled anthropogenic land use change emissions (E_{LUC}). For specified concentrations simulations, the time evolution of H_A (and hence dH_A / dt) is known and using modeled values of F_O and F_L the time evolution of E_F, i.e. the diagnosed fossil fuel emissions, can be estimated. *Arora and Boer* [2010] argue that net LUC emissions (E_{LUC}) are more accurately estimated as the difference in F_L between fully coupled ESM simulations with and without LUC, although a first-order guess is obtained by calculating the amount of biomass deforested.

[6] A 700 year preindustrial control simulation with specified atmospheric CO_2 concentration of 284.7 ppm and 1850 land cover serves as the basis for launching historical simulations. An ensemble of five historical (1850–2005) simulations is performed, which are initialized at 50 year intervals from the preindustrial control. The historical simulation is forced by anthropogenic changes (in CO_2 and non-CO_2 GHGs, aerosols and land cover) as well as the natural variability due to solar variability and explosive volcanoes. Five-member ensemble simulations for the 2006–2100 period are performed for each of the three RCPs (2.6, 4.5, 8.5) which are continuations of the five historical simulations.

3. Results

3.1. Physical Climate

[7] Figure 1a shows time series of the specified atmospheric CO_2 concentration while Figures 1b and 1c show the simulated response of globally averaged screen (2m) temperature and precipitation rates in the control, historical, and RCP-based simulations. The physical surface climate exhibits fairly stationary behavior with virtually no drift in the simulated temperature and precipitation in the control simulation. The ensemble-averaged temperature increase over the historical 1850–2000 period is 0.9°C which compares well the observation-based estimate of 0.76 ± 0.19°C [*Intergovernmental Panel on Climate Change* (*IPCC*), 2007, Figure TS.6]. The net temperature increase over the historical period is determined primarily by a balance between the warming caused by increased GHGs and the cooling associated with increasing aerosols, whose emissions and modelled concentrations plateau near 1980 and then begin to decline (not shown). Explosive volcanoes introduce variability in the simulated historical record as seen by temperature and precipitation reductions around 1883, 1963, and 1991 associated with the Krakatau, Agung and Pinatubo eruptions. The modeled hydrological-cycle strengthens along with an increase in temperature, and warmer temperatures are associated with higher precipitation both for the historical and future periods. For the RCP 2.6, 4.5 and 8.5 scenarios, globally-averaged screen temperature increases by 1.4, 2.3 and 4.9°C, and precipitation increases by 3.6%, 4.5% and 7.8%, over the 2006–2100 period, respectively. The change in precipitation rates are consistent with the competing influences of enhanced GHGs, which reduces the intensity of the hydrologic cycle, and enhanced surface temperatures, which along with higher available energy strengthen the hydrological cycle.

3.2. Biogeochemical Quantities

[8] Simulated atmosphere-land (F_L) and atmosphere-ocean (F_O) CO_2 fluxes, and their cumulative values since 1850, are shown in Figure 2 for all simulations. Unlike the physical climate system variables, F_L and F_O exhibit a small drift (0.053 and −0.067 Pg C/yr, respectively) as seen in the cumulative CO_2 fluxes plot for the control simulation (Figures 2b and 2d). The variability of F_L is higher than that for F_O, consistent with other studies [e.g., *Bousquet et al.*, 2000].

[9] The simulated ensemble-averaged land and ocean CO_2 uptake for the 1850–2005 period are compared with observation-based estimates in Table 1 taking into account the slight drift in the control simulation. The observed change in atmospheric carbon burden (ΔH_A) and cumulative fossil fuel emissions ($\int E_F\, dt$) are based on the CMIP5 data set. Observation-based estimates of cumulative ocean carbon uptake ($\Delta H_O = \int F_O\, dt$) for the 1850–2005 period are based on *Sabine and Feely* [2007] up to 1999 and extended to 2005 using values from *Denman et al*. [2007]. The observed cumulative uptake by land, which is difficult to observe directly, is estimated as the residual ($\Delta H_L = \int E_F\, dt - \Delta H_A - \Delta H_O$) and includes the LUC effect. The simulated historical cumulative ocean uptake ΔH_O (106 Pg C) in the model is somewhat lower than the observation-based estimate of 141 ± 27 Pg C. However, this value may be overestimated by as much as ~7% [*Matsumoto and Gruber*, 2005]. In addition, the observed inventory includes non-trivial contributions from marginal basins and continental shelves which are essentially unresolved and therefore under represented in our model. Simulated change in land carbon $\Delta H_L = \int F_L\, dt$ (which includes the effect of E_{LUC}, see equation (1)) of

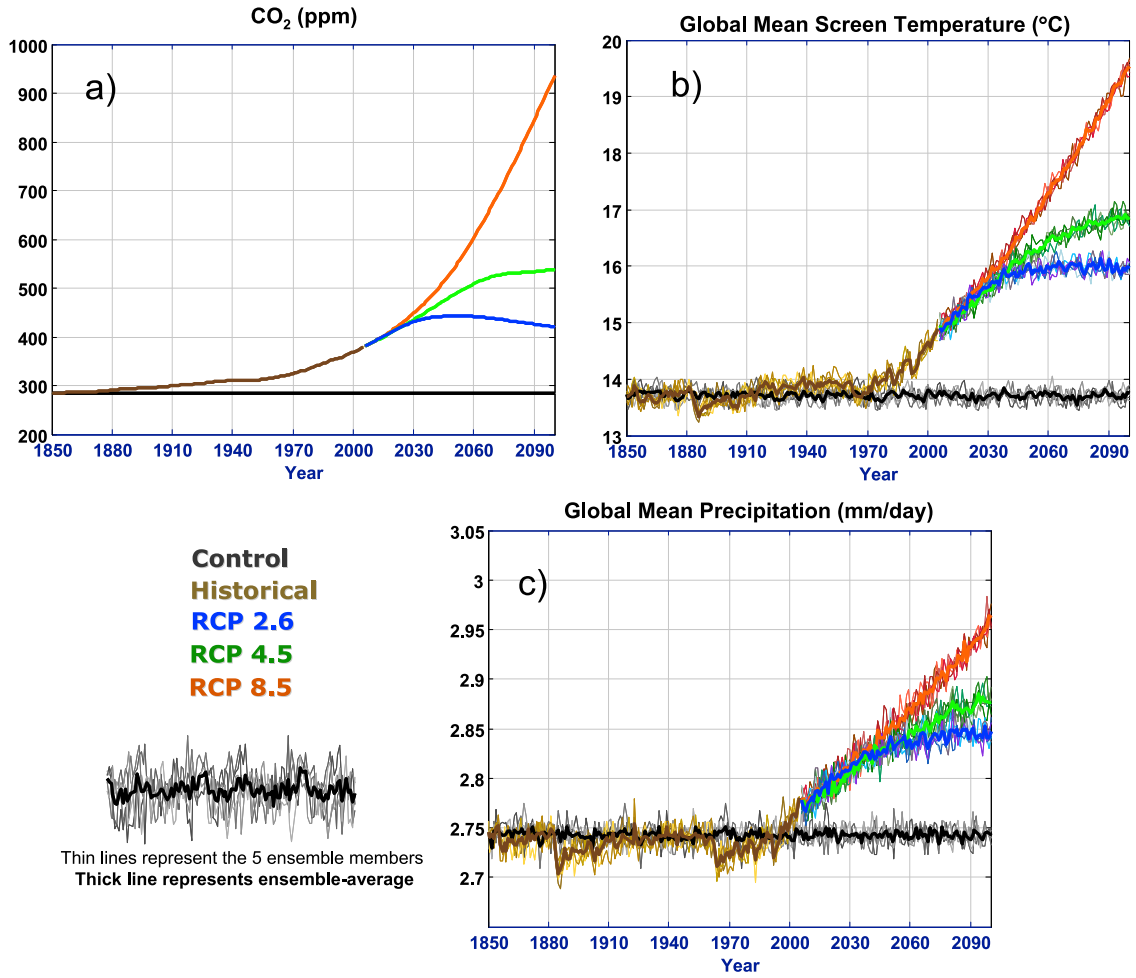

Figure 1. (a) CO_2 concentrations used for the control, historical and the three future RCP-based simulations. (b) Simulated globally-averaged screen (2m) temperature and (c) global mean precipitation rate are also shown for all simulations. The thin lines from control simulation are from the same 700 year long simulation but start at different points along the control simulation corresponding to the points in time from which the individual historical simulations were initialized.

21 Pg C is positive (i.e. carbon uptake by land), and differs from the observation-based residual estimate of −11 ± 47 Pg C in Table 1. This quantity has large uncertainties as also seen in Table 7.1 of *Denman et al*. [2007]. Possible reasons for higher modeled land uptake include a stronger response to temperature reductions associated with volcanic eruptions, lower simulated LUC emissions, and a stronger CO_2 fertilization effect. Two-thirds of the 1850–2005 simulated land carbon uptake has already occurred by about 1940 (Figure 2b) and in simulations with only solar variability and explosive volcanoes (not shown) the ensemble-averaged land uptake is around 23 Pg C suggesting that modeled land uptake in response to temperature reductions associated with volcanic eruptions may be too strong. Simulated deforested biomass in CanESM2 is 65 Pg C over the historical period, or only about half of that estimated by *Houghton* [2008] and therefore could also contribute to higher than observed land uptake (see *Arora and Boer* [2010] for discussion about uncertainty in historical LUC emissions). The combined land and ocean carbon uptake of 127 Pg C, however, compares well with the observation-based estimate of 130 ± 20 Pg C and, consequently, so do the diagnosed cumulative fossil fuel emissions for the 1850–2005 period (327 Pg C compared to 330 ± 20 Pg C observed). The diagnosed emissions during the 1990s (5.2 Pg C/yr) are somewhat lower than observation-based estimate of 6.4 ± 0.4 Pg C/yr (Figure 2e) because of lower carbon uptake by both the land (0.3 compared to 1.0 ± 0.6 Pg C/yr observed [*IPCC*, 2007]) and the ocean (1.6 compared to 2.2 ± 0.4 Pg C/yr observed [*IPCC*, 2007]).

[10] For the 2006–2100 period, simulated ocean carbon uptake is higher than land carbon uptake in all scenarios. Cumulative ocean and land carbon uptake and changes in specified atmospheric carbon burden for this period are summarized in Table 1. Ocean carbon uptake in the three RCP scenarios responds primarily to atmospheric CO_2 concentration with the highest (lowest) uptake occurring for the RCP 8.5 (2.6) scenario. Future land carbon uptake, however, exhibits somewhat different behaviour. Over the 2006–2100 period, while land becomes a source of carbon in the RCP 2.6 scenario, it remains a sink in the RCP 4.5 and 8.5 scenarios with similar cumulative uptake (Table 1). Even though higher CO_2 concentration in the RCP 8.5 scenario yields higher net primary productivity (NPP) than in the RCP 4.5 scenario (not shown), the higher NPP in the

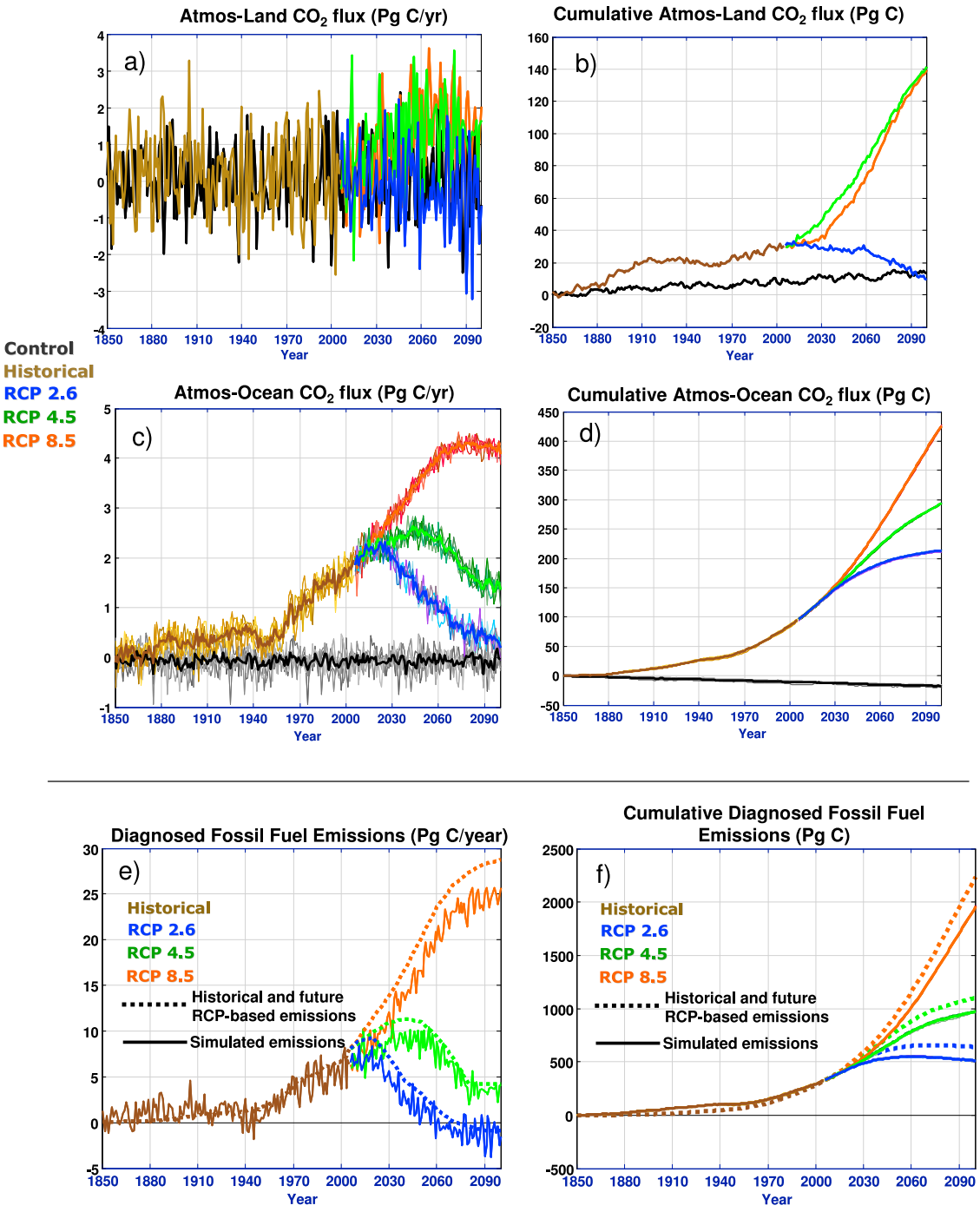

Figure 2. (a) Atmosphere-land flux and (b) its cumulative values and (c) atmosphere-ocean CO_2 flux and (d) its cumulative values for the control, historical and the three future RCP-based simulations In Figures 2c and 2d the thin lines represent individual ensemble members and the thick line their average. For atmosphere-land CO_2 flux and its cumulative values (Figures 2a and 2b), which exhibits large interannual variability, only ensemble-averaged values are shown for clarity. (e) Ensemble-averaged diagnosed fossil fuel emissions for the historical and future period for the three RCPs and (f) their cumulative values. Emissions from the RCP data set are also shown in Figures 2e and 2f.

RCP 8.5 scenario is compensated by higher heterotrophic respiration due to much warmer temperatures over land. The net result is a similar atmosphere-land CO_2 flux in the RCP 4.5 and 8.5 scenarios (Figure 2b and Table 1).

[11] LUC related changes in the land carbon budget are simulated interactively, based on changes in crop area, so the diagnosed emissions represent only fossil fuel emissions (E_F). Cumulative values of deforested biomass are summarized in Table 1. In any case, except for RCP 2.6, crop area changes over the 2006–2100 period represent only a small fraction of the historical 1850–2005 change leaving fossil fuel emissions as the dominant driver of environmental

Table 1. Specified Change in Atmospheric CO_2 Burden, Simulated Changes in Land and Ocean Carbon, and Diagnosed Fossil Fuel Emissions for the 1850–2005 and 2006–2100 Periods[a]

	Observation-Based	Model-Simulated	
1850–2005			
Change in atmospheric CO_2 burden (ΔH_A)	200	200 (specified)	
Change in ocean carbon (ΔH_O)	141 ± 27	106	
Change in land carbon (estimated as residual of other quantities) (ΔH_L)	−11 ± 47	21	
Change in land plus ocean carbon ($\Delta H_L + \Delta H_O$)	130 ± 20	127	
Cumulative fossil fuel plus biofuel emissions ($\int E_F\, dt$)	330 ± 20	327 (diagnosed)	
	RCP 2.6	RCP 4.5	RCP 8.5
2006–2100			
Specified change in atmospheric CO_2 burden (ΔH_A)	85	334	1177
Change in ocean carbon (ΔH_O)	123	203	336
Change in land carbon (ΔH_L)	−26	106	104
Change in land plus ocean carbon ($\Delta H_L + \Delta H_O$)	97	309	440
Cumulative deforested biomass	60	7	33
Cumulative diagnosed fossil fuel emissions ($\int E_F\, dt$)	182	643	1617
Cumulative fossil fuel emissions from RCPs ($\int E_F\, dt$)	321	785	1918
1850–2100			
Cumulative diagnosed fossil fuel emissions ($\int E_F\, dt$) plus deforested biomass	634	1042	2042
Cumulative diagnosed fossil fuel emissions ($\int E_F\, dt$)	509	970	1944
Cumulative historical observation-based plus future RCP-based fossil fuel emissions ($\int E_F\, dt$)	640	1104	2237

[a]Modeled values are corrected for the drift in the control simulation. Values for the 1850–2005 period are compared with observation-based values. The 2006–2100 period values are shown for the three RCPs. Cumulative diagnosed fossil fuel emissions (plus deforested biomass) values are also shown for the full 1850–2100 period. Units are Pg C. The uncertainty in change in the ocean carbon values for the historical period is based on [*Sabine and Feely* 2007] for estimates up to 1999 so in principle could be higher than ±27 Pg C. The cumulative emissions for the historical period are the sum of 319.5 Pg C of fossil fuel emissions and 10.5 Pg C of biofuel emissions which are estimated as explained by *Arora et al*. [2009]. The uncertainty in fossil fuel emissions is ±6% based on http://www.globalcarbonproject.org/carbonbudget/08/hl-full.htm.

change in the future. Ensemble-averaged drift-corrected diagnosed fossil fuel emissions, and their cumulative values, for the historical period and the three future RCPs are shown in Figures 2e and 2f. The control simulation drifts in F_L and F_O are of opposite sign and nearly cancel each other. Consequently, the drift correction for diagnosed emissions is small (−0.01 Pg C/yr). Diagnosed fossil fuel emissions (E_F) are compared with those provided in the RCP data set itself, i.e. for emissions driven simulations (dotted lines in Figures 2e and 2f). Cumulative diagnosed fossil fuel emissions ($\int E_F\, dt$) from CanESM2 and the RCP data set, for the 2006–2100 period, are summarized in Table 1. CanESM2 diagnosed fossil fuel emissions are lower than those in the RCP data set for all scenarios. This is consistent with the inclusion of explicit carbon-climate feedbacks in our simulations, which reduce the sink capacity of the land and the ocean. Such feebacks are absent in the integrated assessment models (IAMs) which use simplified carbon cycle models. It is anticipated that the diagnosed emissions from participating models in the CMIP5 will vary over a wide range of values due to the relative strengths of their carbon-climate feedbacks. Of all the RCP scenarios, RCP 2.6 is the most aggressive, in terms of required emissions reduction, with atmospheric CO_2 concentration of just above 420 ppm in 2100 (i.e. only ~33 ppm higher than the 2009 value of 387 ppm). Both CanESM2 derived and RCP-based fossil fuel emissions for this scenario suggest that emissions must start decreasing immediately and that emissions must become negative by roughly 2060 and remain so (i.e. ongoing carbon sequestration). A similar pattern of decreasing emissions is obtained by *Roeckner et al*. [2010] for a RCP 2.6 like scenario (their E1 scenario) but with much higher cumulative emissions primarily due to their stronger land carbon sink over the 21st century, than CanESM2. This is likely associated with lower temperature sensitivity of soil carbon in their model [*Arora and Matthews*, 2009].

4. Discussion and Conclusions

[12] The concept of proportionality between temperature change caused by CO_2 increase and cumulative carbon emissions has recently gained attention [*Matthews et al.*, 2009] as a potentially useful policy tool. Values for this CO_2 induced temperature change per unit cumulative CO_2 emissions (i.e. the carbon-climate response, CCR) vary in the range 1.0 – 2.1 °C/Eg C (1 Eg = 10^{18} g) for C^4MIP models [*Matthews et al.*, 2009]. For CanESM2 in the standard experiment where CO_2 increases at 1% per year (compounded) to a level four times that of the preindustrial climate (not shown), the CCR at the end of the simulation is 1.7 °C/Eg C, consistent with C^4MIP models. However, for the results presented here the temperature change per unit cumulative CO_2 emissions (diagnosed fossil fuel emissions plus amount of deforested biomass), for the 1850–2100 period, is 3.6, 3.1 and 2.8 °C/Eg C for the RCP 2.6, 4.5 and 8.5 scenarios. The reason for these larger values in CanESM2 is that the effects of non-CO_2 GHGs and aerosols, which were excluded in the C^4MIP, are included in our simulations (as part of their specification in the RCP data set). In CanESM2, the combined impact of non-CO_2 GHGs and aerosols is negligible over the historical period 1850–2000. Over the period 2001–2100, however, the impact of non-CO_2 GHGs dominates that of aerosols resulting in an additional warming of 0.6, 0.8 and 1.7 °C in the RCP 2.6, 4.5 and 8.5 scenarios, respectively. This additional warming reduces the sink capacity of the land and the oceans resulting in

lower fossil-fuel carbon emissions determined for a given CO_2 concentration pathway. The significant impact of non-CO_2 GHGs and aerosols limits the ability of CCR to quantify future allowable emissions.

[13] The cumulative emissions (diagnosed fossil fuel emissions plus deforested biomass) over the 1850–2100 period for the RCP 2.6 scenario in CanESM2 are 634 Pg C (Table 1). The corresponding warming is 2.3°C over this period, which is slightly larger than the 2°C threshold set by the 2009 UN Copenhagen Accord to avoid dangerous climate change. Diagnosed cumulative carbon emissions in studies ignoring the effect of non-CO_2 GHGs are, as expected, higher. For example, *Allen et al*. [2009] estimate cumulative emissions of 1000 Pg C for 2°C warming above pre-industrial using the Hadley Centre Simple Carbon-Climate-Cycle Model assuming that the future temperature responses of aerosols and non-CO_2 GHGs cancel each other. Since observation-based estimates of cumulative fossil fuel plus LUC emissions up to 2005 are 476 ± 78 Pg C (CMIP5 fossil fuel emissions plus Houghton's LUC emissions with ±50% uncertainty), our results suggest there is little room (~160 ± 80 Pg C) to limit the warming in 2100 to the 2.3°C associated with the RCP 2.6 concentration scenario. It would require an immediate and rapid ramp down of emissions, followed by negative emissions (sequestration) in the later half of this century (Figure 2e). Based on CanESM2 results, achieving the 2°C warming target, as opposed to 2.3°C obtained for RCP 2.6, requires a further reduction in cumulative emissions of roughly 180 Pg C (i.e. the additional 0.3°C divided by CanESM2's CCR value of 1.7 °C/Eg C). This implies that we have already surpassed the cumulative emission limit and so emissions must ramp down to zero immediately. The unprecedented reduction in fossil-fuel emissions implied by either of these scenarios suggests that it is unlikely that warming can be limited to the 2°C target agreed to in the 2009 Copenhagen Accord.

[14] **Acknowledgments.** The authors thank John Fyfe, Nathan Gillett, and one anonymous reviewer for providing useful comments.

References

Allen, M. R., D. J. Frame, C. Huntingford, C. D. Jones, J. A. Lowe, M. Meinshausen, and N. Meinshausen (2009), Warming caused by cumulative carbon emissions towards the trillionth tonne, *Nature*, *458*, 1163–1166, doi:10.1038/nature08019.

Arora, V. K., and G. J. Boer (2010), Uncertainties in the 20th century carbon budget associated with land use change, *Global Change Biol.*, *16*(12), 3327–3348, doi:10.1111/j.1365-2486.2010.02202.x.

Arora, V. K., and H. D. Matthews (2009), Characterizing uncertainty in modeling primary terrestrial ecosystem processes, *Global Biogeochem. Cycles*, *23*, GB2016, doi:10.1029/2008GB003398.

Arora, V. K., G. J. Boer, J. R. Christian, C. L. Curry, K. L. Denman, K. Zahariev, G. M. Flato, J. F. Scinocca, W. J. Merryfield, and W. G. Lee (2009), The effect of terrestrial photosynthesis down-regulation on the 20th century carbon budget simulated with the CCCma Earth System Model, *J. Clim.*, *22*, 6066–6088, doi:10.1175/2009JCLI3037.1.

Bousquet, P., et al. (2000), Regional changes in carbon dioxide fluxes of land and ocean since 1980, *Science*, *290*, 1342–1346, doi:10.1126/science.290.5495.1342.

Christian, J. R., et al. (2010), The global carbon cycle in the Canadian Earth system model (CanESM1): Preindustrial control simulation, *J. Geophys. Res.*, *115*, G03014, doi:10.1029/2008JG000920.

Denman, K. L., et al. (2007), Couplings between changes in the climate system and biogeochemistry, in *Climate Change 2007: The Physical Science Basis. Contribution of Working Group I to the Fourth Assessment Report of the Intergovernmental Panel on Climate Change*, edited by S. Solomon et al., pp. 499–587, Cambridge Univ. Press, Cambridge, New York.

Hibbard, K. A., G. A. Meehl, P. M. Cox, and P. Friedlingstein (2007), A strategy for climate change stabilization experiments, *Eos Trans. AGU*, *88*(20), doi:10.1029/2007EO200002.

Houghton, R. A. (2008), Carbon flux to the atmosphere from land-use changes: 1850–2005, in *TRENDS: A Compendium of Data on Global Change*, Carbon Dioxide Inf. Anal. Cent., Oak Ridge Natl. Lab., Oak Ridge, Tenn., doi:10.3334/CDIAC/lue.ndp050.

Intergovernmental Panel on Climate Change (2007), *Climate Change 2007: The Physical Science Basis. Contribution of Working Group I to the Fourth Assessment Report of the Intergovernmental Panel on Climate Change*, edited by S. Solomon et al., Cambridge Univ. Press, Cambridge, New York.

Matsumoto, K., and N. Gruber (2005), How accurate is the estimation of anthropogenic carbon in the ocean? An evaluation of the ΔC* method, *Global Biogeochem. Cycles*, *19*, GB3014, doi:10.1029/2004GB002397.

Matthews, H. D., N. P. Gillett, P. A. Stott, and K. Zickfeld (2009), The proportionality of global warming to cumulative carbon emissions, *Nature*, *459*, 829–832, doi:10.1038/nature08047.

Roeckner, E., M. A. Giorgetta, T. Cueger, M. Esch, and J. Pongratz (2010), Historical and future anthropogenic emission pathways derived from coupled climate-carbon cycle simulations, *Clim. Change*, doi:10.1007/s10584-010-9886-6, in press.

Sabine, C. L., and R. A. Feely (2007), The oceanic sink for carbon dioxide, in *Greenhouse Gas Sinks*, edited by D. S. Reay et al., pp. 31–49, CABI, Cambridge, Mass, doi:10.1079/9781845931896.0031.

Scinocca, J. F., N. A. McFarlane, M. Lazare, J. Li, and D. Plummer (2008), Technical Note: The CCCma third generation AGCM and its extension into the middle atmosphere, *Atmos. Chem. Phys.*, *8*, 7055–7074, doi:10.5194/acp-8-7055-2008.

V. K. Arora, G. J. Boer, J. R. Christian, K. L. Denman, G. M. Flato, V. V. Kharin, W. G. Lee, W. J. Merryfield, and F. Scinocca, Canadian Centre for Climate Modelling and Analysis, Environment Canada, University of Victoria, Victoria, BC V8W 2Y2, Canada. (Vivek.Arora@ec.gc.ca)